

# **Aqueous-Based Extrusion Fabrication of Ceramics on Demand**

Michael S. Mason<sup>1</sup>, Tieshu Huang<sup>1</sup>, Robert G. Landers<sup>1</sup>,  
Ming C. Leu<sup>1</sup>, Gregory E. Hilmas<sup>2</sup>, and Michael W. Hayes<sup>3</sup>

1870 Miner Circle  
Department of Mechanical and Aerospace Engineering<sup>1</sup>  
Department of Materials Science and Engineering<sup>2</sup>  
University of Missouri-Rolla, Rolla, Missouri 65409-0050  
The Boeing Company<sup>3</sup>, St. Louis, Missouri  
{mmason,hts,landersr,mleu,ghilmas}@umr.edu  
michael.w.hayes2@boeing.com

**Reviewed, accepted September 4, 2007**

## **ABSTRACT**

Aqueous-Based Extrusion Fabrication is an additive manufacturing technique that extrudes ceramic slurries of high solids loading layer by layer for part fabrication. The material reservoir in a previously developed system has been modified to allow for starting and stopping of the extrusion process on demand. Design pros and cons are examined and a comparison between two material reservoir designs is made. Tests are conducted to determine the optimal deposition parameters for starting and stopping the extrudate on demand. The collected test data is used for the development of a deposition strategy that improves material deposition consistency, including reduced material buildup at sharp corners. Example parts are fabricated using the deposition strategy and hardware design.

## **INTRODUCTION**

Aqueous based extrusion fabrication (ABEF) of ceramics is a Solid Freeform Fabrication (SFF) process that deposits ceramic paste layer by layer through extrusion. The process has been previously introduced, and details regarding the build material and equipment can be found in [1-3]. A process schematic and photograph of the system are shown in Figures 1 and 2, respectively. The material deposition device previously developed gave good results for continuous material deposition. The ability to start and stop the material extrusion on demand was not yet developed in our previous work. With the need to be able to fabricate more complex geometries, different extrusion processes were surveyed for the process of starting/stopping material deposition on demand. The first system surveyed was the Fused Deposition of Ceramics (FDC) process, which modified a Fused Deposition Modeling (FDM) machine to deposit a ceramic/polymer fiber strand [4-5]. The FDM process uses two rollers with heaters to move the material fiber either forward for deposition or in reverse to stop the deposition. The second process uses a Micro-Scale Robotic Deposition System [6], which was based on the Robocasting process developed by Sandia National Laboratories [7-8]. This process uses air pressure to extrude material for deposition and uses one-way control valves for starting and stopping of the extrusion process. These “retraction” processes can be applied to the ABEF system by retreating the ram extruder from touching the material

reservoir plunger. This would in theory reduce the applied pressure, thereby stopping material extrusion.

In this paper material deposition tests are conducted, where the ram extruder retreating velocity is varied in order to develop a technique that can be used for starting/stopping the extrusion process on demand. A new extrusion mechanism is designed to improve process capabilities. Parts are then fabricated with the use of starting/stopping the extrusion on demand with emphasis being placed on deposition of sharp corners and edges.

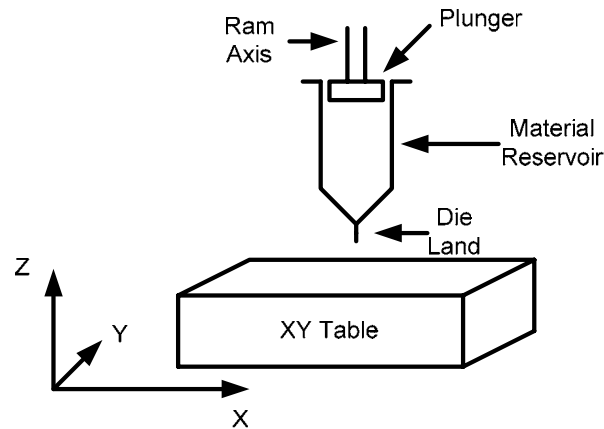


**Figure 1: Schematic showing the location of the die land for an extrusion nozzle.**

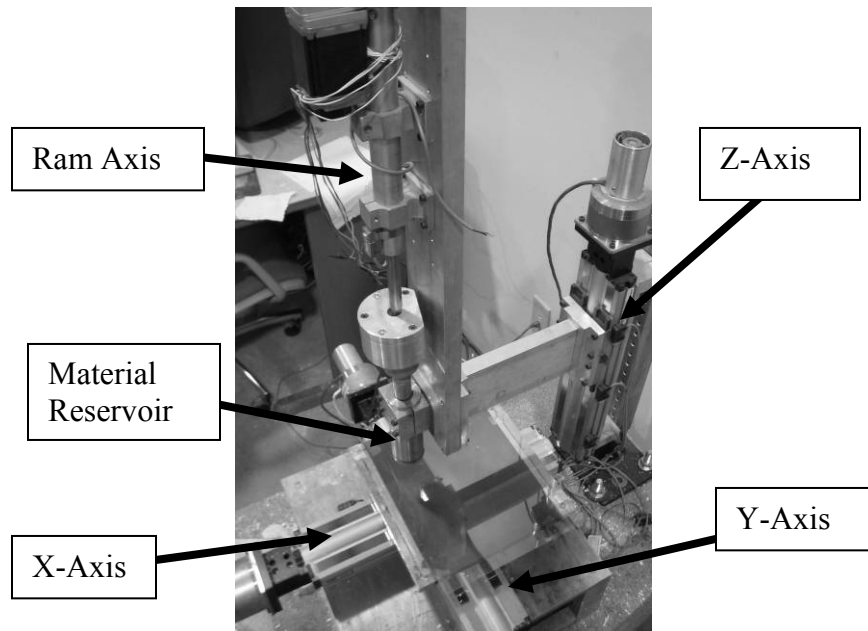


**Figure 2: Photograph of the ABEF system used in this study.**

### STOPPING MATERIAL FLOW TESTING

Experiments were conducted to test the feasibility of stopping material deposition on demand by retreating the ram extruder. The schematic of the original extrusion mechanism utilizing a plastic syringe and hypodermic needles is shown in Figure 3. Single lines were deposited at table velocities of 25 mm/s and 30 mm/s with a desired ram force of 308 N at a standoff distance of 150  $\mu\text{m}$ . These process parameters yielded good deposition as determined from previous part fabrication using the original extrusion mechanism. Once the table velocity has reached a steady state and traveled a fixed distance (5 mm), the ram was retreated at a given velocity ranging 0-10 mm/s. After the ram is retreated the amount of excess material deposited was measured from the desired stopping location. Figure 4 shows the deposition length for table velocities of 25 mm/s and 30 mm/s. By examining Figure 4 it can be seen that the extrusion is not able to stop on demand, regardless of the ram retreating velocity. This is due to the fact that the ram axis is not directly connected to the plunger (see Figure 3). When the ram retreats it does not directly stop the pressure being applied to the fluid within the plastic syringe. It only detaches itself from the plunger. In order for the material to stop extruding, equilibrium must be reached between the applied extrusion force and the shear stress created by fluid motion. This occurs when enough material has been released, decreasing the amount of material present within the same material reservoir volume. From these results the ram retreating method of stopping the extrusion process was not a viable solution with the plastic syringe extrusion mechanism design.

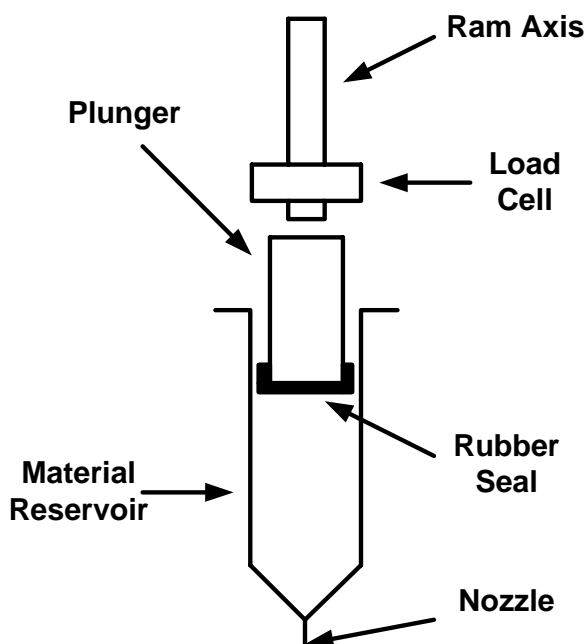


**Figure 3: Schematic of original extrusion mechanism utilizing a plastic syringe and hypodermic needles.**

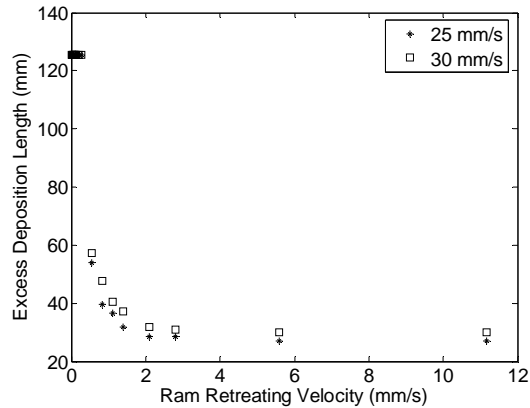


**Figure 4: Ram retreating test data for the original extrusion mechanism.**

### NEW EXTRUSION MECHANISM DESIGN

In order to improve the process by adding the ability to stop the extrusion on demand, a new extrusion mechanism was designed on the basis that to stop the extrusion it would be necessary to retract not only the ram axis but also the plunger. To accomplish this, a housing was placed around the load cell that would connect directly to the plunger. With the load cell enclosed as the ram axis is retreated the load cell touches the housing, thereby raising the plunger. A schematic of the new design is shown in Figure 5.

To further improve the system it was decided to replace the plastic syringe and hypodermic needles with a two-piece metal reservoir. The metal reservoir reduces variability in the internal pressure that was present in the original extrusion mechanism due to expansion of the plastic syringe. The mechanical design is such that different dies can be used for the desired material deposition height and width.

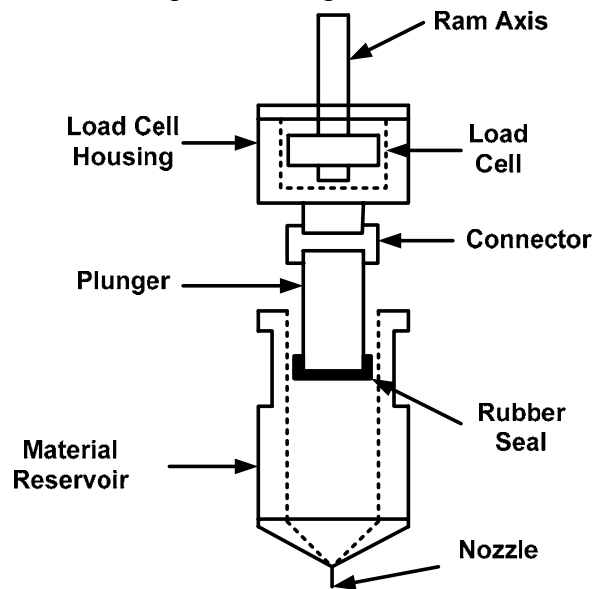


**Figure 5: Schematic of new extrusion mechanism utilizing an interlocking system made of 304 stainless steel.**

To determine a suitable design for a new material reservoir the resulting stress on the reservoir was calculated using

$$\sigma = \frac{F}{A} = \frac{F}{\pi(R_o^2 - R_i^2)} \quad (1)$$

where  $\sigma$  is the axial stress acting on the system,  $F$  is the extrusion force,  $A$  is the equivalent area, and  $R_o$  and  $R_i$  are the outer and inner radii of the reservoir, respectively. Substituting in the values of  $F = 4.4 \text{ kN}$  (maximum extrusion force),  $R_o = 15.2 \text{ mm}$ , and  $R_i = 12.7 \text{ mm}$ , the maximum axial stress is determined to be  $\sigma = 63 \text{ MPa}$ . In order to guarantee the reservoir would not fail under this stress the wall thickness was increased to  $12.5 \text{ mm}$  and 304 stainless steel was chosen for its yield stress of  $500 \text{ MPa}$ . With these changes made, a factor of safety of 7.9 is present in the design. Figure 6 shows the newly designed material reservoir as implemented into the ABEF system. For the design of the nozzle, a diameter of  $0.5 \text{ mm}$  was chosen as a similar diameter ( $580 \text{ }\mu\text{m}$ ) to that previously used with the plastic syringe and a die land length of  $5 \text{ mm}$  was chosen, which was a 50% reduction in length from the previously used hypodermic needles. Figure 7 shows a close-up view of the die land of the new reservoir. Tests proved that the new design worked without failure.

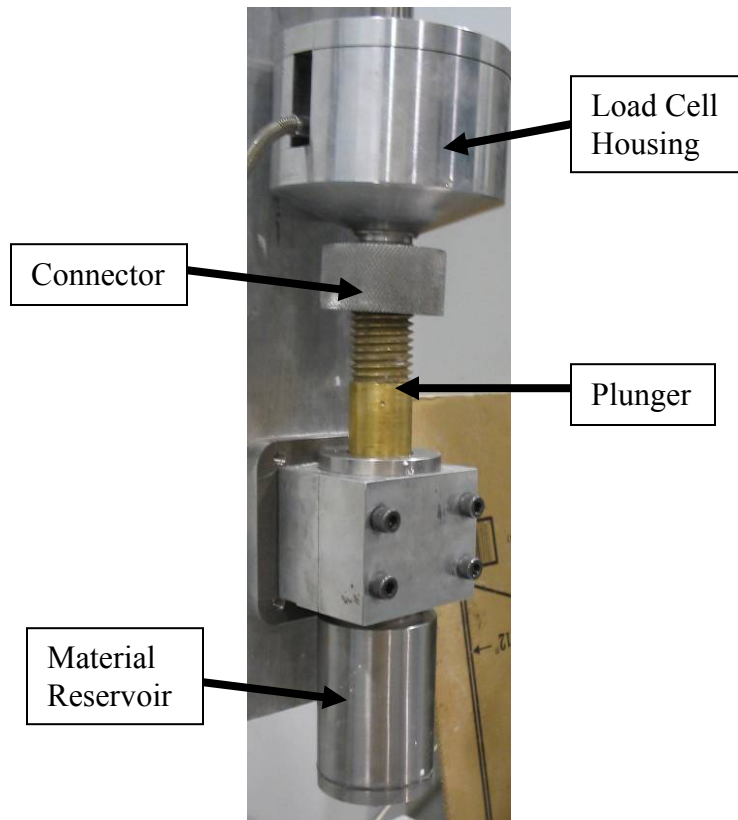


**Figure 6: 304 stainless steel extrusion mechanism design implemented in the ABEF system.**

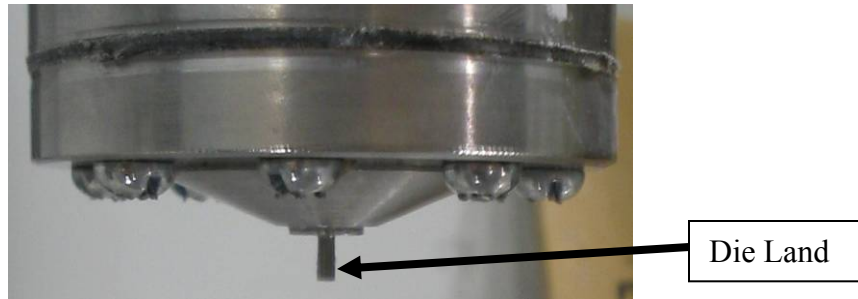


**Figure 7: Picture of new extrusion mechanism die land.**

The ram retreating experiments were repeated using the new extrusion mechanism. Three different extrusion forces were used: 308, 445, and 582 *N*. These extrusion forces were chosen due to good deposition results during part fabrication using the original extrusion mechanism. Figure 8 shows the results from the deposition tests using the new extrusion mechanism. The extrusion was able to be stopped on demand using the retreating method at all three extrusion forces. There was an exponential decrease in the amount of excess deposition as the retreating velocity increased for all extrusion forces.

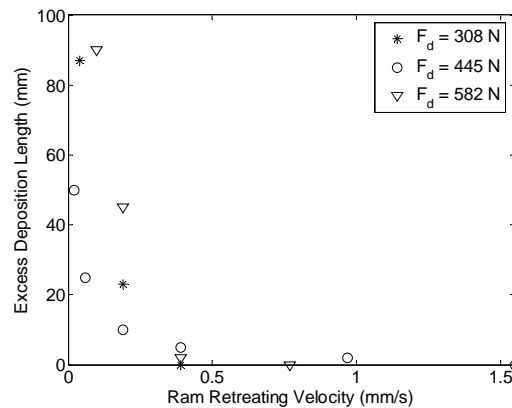


**Figure 8: Ram retreating results using the new extrusion mechanism with a table velocity of 25 *mm/s* and a standoff distance of 0.5 *mm*.**

In order to determine the repeatability of stopping the extrusion process, the line deposition tests were conducted 10 times for ram retreating velocities of 0, 0.25, 0.5, 1, 1.5, 2, 2.5, and 3 *mm/s* at an extrusion force of 308 *N*. Standard deviations of 0.0, 9.2, 1.5, 4.7, 1.0, 0.0, 0.0, and 0.0 *mm* were calculated for the ram retreating velocities, respectively. Figures 9-12 show pictures of the line deposition tests at ram retreating velocities of 0.5, 1, 1.5, and 2 *mm/s*, respectively. Velocities higher than 2 *mm/s* were also able to stop the extrusion on demand. From the figures it can be seen that the process is repeatable, with small variations in excess deposition between individual runs at a given ram retreating velocity. Once the ram begins to retreat, the deposited lines decrease in thickness until gaps become present in the deposition. The gapped deposition is due to the reduction in extrusion force. As the extrusion force decreases the ceramic

paste extrudes slower and slower eventually not being able to keep up with the table velocity causing the material to shear thereby causing gaps in the deposition. Figure 13 shows the results from the repeatability tests.

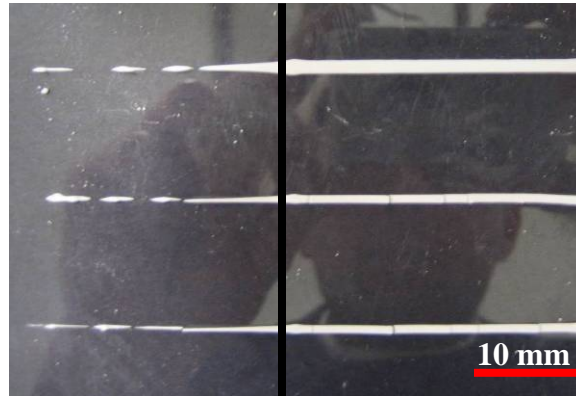


**Figure 9:** Three runs of line depositions with ram retreating velocity of  $0.5 \text{ mm/s}$  and  $F_d = 308 \text{ N}$ . Black line indicates desired stopping location.

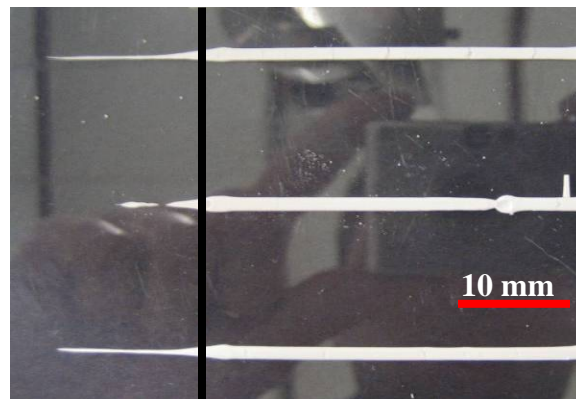


**Figure 10:** Three runs of line depositions with ram retreating velocity of  $1 \text{ mm/s}$  and  $F_d = 308 \text{ N}$ . Black line indicates desired stopping location.

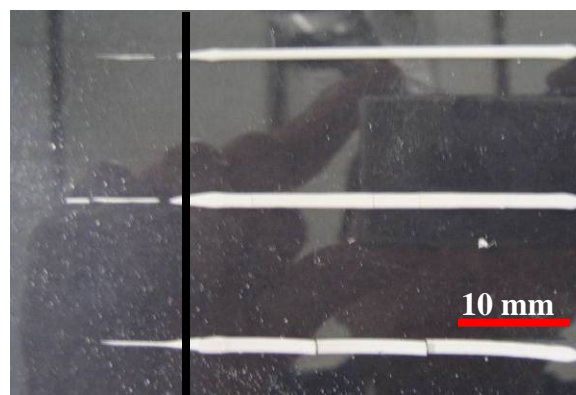


**Figure 11:** Three runs of line depositions with ram retreating velocity of  $1.5 \text{ mm/s}$  and  $F_d = 308 \text{ N}$ . Black line indicates desired stopping location.

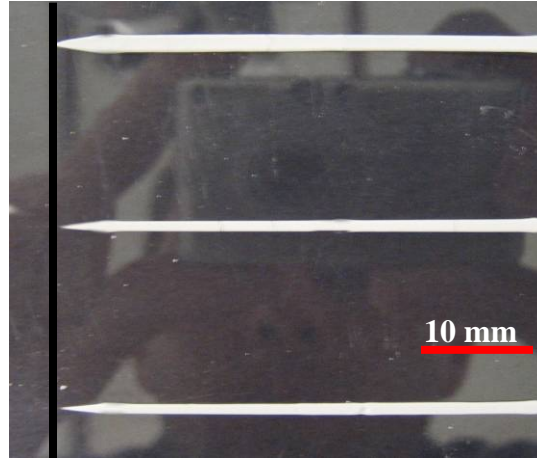


**Figure 12: Three runs of line depositions with ram retreating velocity of 2 mm/s and  $F_d = 308 N$ . Black line indicates desired stopping location.**

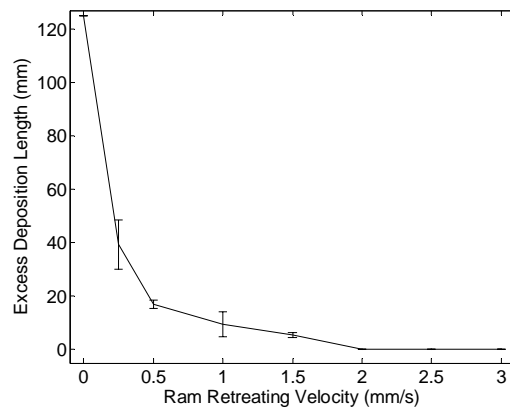


**Figure 13: Chart of retreating test data at a table velocity of 25 mm/s,  $F_d = 308 N$ , and a standoff distance of 0.5 mm. Error bars represent one standard deviation.**

### PART FEATURES

With the ability to stop the extrusion on demand, the next objective was to test this technique for part fabrication. The first part used for testing was a single layer square with an interior rectangular hole. In order to fabricate this part a motion path as shown in Figure 14 was used. First the exterior contour was deposited for a smooth outer surface. Next the interior was deposited in a rastering motion. The black lines in Figure 14 indicate material deposition and the gray lines indicate no deposition. Figure 15 shows the fabricated part. The desired deposition dimensions of the part were 25 mm X 25 mm with a 10 mm X 10 mm interior square hole. Ten separate measurements were taken of each dimension after freeze drying to allow the part to reach brown state. Measurements are taken in the brown state due to the deposited material having a very low yield stress before drying, allowing for easy deformation during measurement. The average length parallel to deposition was 24.2 mm and the average length perpendicular to deposition was 24.8 mm with standard deviations of 0.4 and 0.6 mm, respectively.



This yields a dimensional error of 3.2% and 0.8% for the parallel and perpendicular dimensions, respectively, after freeze drying. The interior hole was 11.1 *mm* parallel to deposition and 11.5 *mm* perpendicular to deposition with standard deviations of 0.24 and 0.3 *mm*, respectively. The dimensional error for the internal holes is 11.1% and 15% for the parallel and perpendicular deposition directions, respectively. The error present between the desired and actual dimensions is due to the shrinkage of the part during the freeze drying stage. The differences in size between the parallel and perpendicular measurements are caused by different drying rates of the part. When the part is drying, the parallel deposition direction is allowed to dry more uniformly with all of the deposition ends open to the environment as opposed to the perpendicular direction having only a single line open to the environment for drying. The larger amount of error present in the internal measurement was due to shrinkage in two directions as compared to the single direction with the external dimensions.

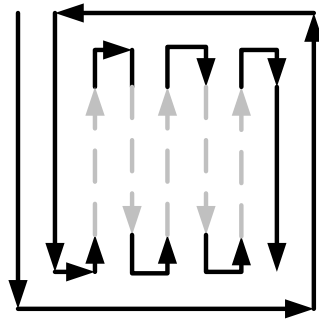


**Figure 14: 2D test part motion path. Dashed lines indicate no deposition.**

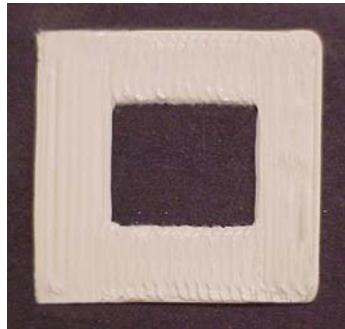


**Figure 15: Top view of deposited material from motion path in Figure 14 at a table velocity of 15 *mm/s*, standoff distance of 0.5 *mm*, and  $F_d = 308$  *N*.**

With the success of being able to fabricate 2-dimensional shapes by starting and stopping the extrusion on demand, the described technique was implemented for the fabrication of 3-dimensional parts. The part fabricated in this test was a slanted block with an interior hole. The same motion path is followed as for the 2D part, but between layers a 200  $\mu\text{m}$  shift is made in both the X and Y directions. Figures 16 and 17 show the side and top view, respectively. As can be seen from Figure 16 some curling is present at the edges of the part. This is caused by the uneven drying rate of the part in room

temperature. The first couple of layers dry quickly compared to the remaining layers. The internal layers are enclosed from the external environment, allowing for more uniform drying.

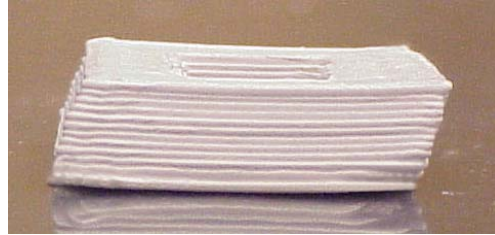


**Figure 16: Side view of slanted part at a table velocity of 15 mm/s, standoff distance of 0.5 mm, and  $F_d = 308$  N.**

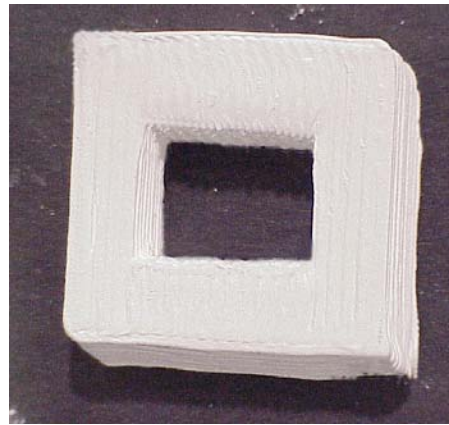


**Figure 17: Top view of part in Figure 16.**

### **SUMMARY AND CONCLUSIONS**

A new extrusion mechanism for the process of aqueous-based extrusion fabrication of high solids loading ceramics on demand has been designed and implemented, providing an extrusion capability that cannot be done with the use of a plastic syringe for extrusion. Deposition tests were conducted to examine the relationship between ram retreating velocity and excess material deposition. There is an exponential decrease of excess material deposition with increasing ram retreating velocity. The implementation of the new extrusion mechanism allows for the extrusion to start and stop as programmed. The ability to start and stop the extrusion on demand allows for more complex 3D part fabrication including sharp corners and features. Parts were fabricated using the new material reservoir to demonstrate the developed capability. Several features were measured for dimensional accuracy compared to desired dimensions. More shrinkage was present in the parallel deposition areas than the perpendicular deposition areas due to a more even area present for drying. The exterior part dimensions were more accurate than interior due to less surface area for drying.

## ACKNOWLEDGEMENT

This work was supported by the Air Force Research Laboratory under Contract FA8650-04-C-5704.

## REFERENCES

1. Huang, T., Mason, M., Hilmas, G.E., and Leu, M.C., 2006, "Freeze-Form Extrusion Fabrication of Ceramic Parts," *International Journal of Virtual and Physical Prototyping*, Vol. 1, No. 2, pp. 93-100.
2. Huang, T., Mason, M., Hilmas, G.E., and Leu, M.C., 2006, "Freeze-Form Extrusion Fabrication of Ultra High Temperature Ceramics," *Materials Science and Technology Conference*, Cincinnati, Ohio, October 15-19.
3. Mason, M., Huang, T., Landers, R., Leu, M.C., and Hilmas, G., 2006, "Freeform Extrusion of High Solids Loading Ceramic Slurries, Part I: Extrusion Process Modeling," *Proceedings of Solid Freeform Fabrication Symposium*, Austin, Texas, August 14-16.
4. Jafari, M. A., Han, W., Mohammadi, F., Safari, A., Danforth, S.C., and Langrana, N., 2000, "A Novel System for Fused Deposition of Advanced Multiple Ceramics," *Rapid Prototyping Journal*, Vol. 6, No. 3, pp. 161-174.
5. Qui, D., Langrana, N.A., Danforth, S.C., Safari, A., and Jafari, M., 2001, "Intelligent Toolpath Extrusion-Based LM Process," *Rapid Prototyping Journal*, Vol. 7, No. 1, pp. 18-23.
6. Mukhopadhyay, S., Bristow, D.A., and Ferreira, P.M., 2005, "Multi-Material Micro-scale Robotic Deposition," *Proceedings of the 2005 IERC*, Atlanta, Georgia, May 14-18.
7. Cesarano, J. and Calvert, P., US Patent 6,027,326.
8. Cesarano, J., Segalman, R., and Calvert, P., 1998, "Robocasting Provides Moldless Fabrication from Slurry Deposition," *Ceramic Industry*, pp. 94-102.